Approximate solution of the classical Liouville equation using Gaussian phase packet dynamics: Application to enhanced equilibrium averaging and global optimization

Jianpeng Ma, D. Hsu,[a] and John E. Straub
Department of Chemistry, Boston University, Boston, Massachusetts 02215

(Received 9 February 1993; accepted 14 May 1993)

An approximate method for integrating the Liouville equation to obtain the time-dependent classical phase space density distribution at constant energy or temperature is presented. The density distribution of each degree of freedom is represented by a single Gaussian phase packet (GPP) whose center and width obey variationally optimized equations of motion. The constant energy dynamics is applied to the calculation of equilibrium thermodynamic averages for a Lennard-Jones cluster and fluid to demonstrate the feasibility and utility of this approximate method for the simulation of many-body condensed phase systems. The rate of kinetic energy equipartitioning is examined for GPP dynamics using a generalization of the ergodic measure and found to be significantly faster than for standard molecular dynamics simulation. A global optimization algorithm is developed based on simulated annealing of the phase space density distribution. This method is applied to the global energy minimization of Lennard-Jones clusters and found to be superior to simulated annealing methods employing classical point particles.

I. INTRODUCTION

The successes of molecular dynamics computer simulation in exploring the properties of condensed phase systems such as liquids,[1] glasses, and biomolecules[2,3] are well known. However, in recent years, it has become clear that the solution to many questions, such as exhaustive phase space sampling in nonergodic glassy systems or biomolecules, is at present beyond the reach of computer simulation due to the ruggedness of the potential energy landscape and the enormous range of time scales involved.[4] This point has been made most beautifully in the inherent structure theory of Stillinger and co-workers for liquids and glasses[5] and the conformational substates model of Frauenfelder and co-workers for biomolecules.[6] The difficulties facing existing methods lie in the need to overcome energy barriers much larger than the thermal energy on a computationally accessible time scale and in the need to follow accurately high frequency vibrations against a background of low frequency motion. Both problems are detrimental to good statistical sampling of relevant conformation space given a finite amount of computer time. One solution is to extend the reach of computer simulation using yet more powerful computers. Another, complementary approach is to employ enhanced sampling algorithms which improve the statistics by lowering the barriers through a coarse graining of the conformational space.[7]

In this paper, we propose an enhanced sampling algorithm based on the approximate integration of the classical Liouville equation for the time evolution of the phase space density distribution. By integrating the classical density distribution, we replace the calculation of a single trajectory, which explores points in phase space, with a continuum of trajectories, which explore entire volumes of phase space at once. We find that the sampling statistics are improved over those of standard molecular dynamics with only a modest increase in effort. In addition, the density distribution moves on an energy surface that is the potential energy averaged over the distribution. This averaged surface is smoother than the bare potential surface. The averaging over the density distribution in effect raises energy minima and lowers energy barriers.

Our approach to the classical Liouville equation draws on the formal equivalence of this equation to the time-dependent Schrödinger equation.[8] Gaussian wave packets, first popularized by Heller[9,10] for integrating the time-dependent Schrödinger equation, have also been applied to the calculation of spectroscopic correlation functions using the von Neumann (quantum Liouville) equation.[11–14] Mukamel and co-workers observed that the equations of motion for a Gaussian approximation to the density matrix can be adapted to classical mechanics by replacing the quantum Liouville operator and density matrix with the classical Liouville operator and phase space density distribution.[13] Here we apply this formalism to the Liouville equation for the simulation of classical many-body systems.[15,16] The classical density distribution of each particle is represented by a single Gaussian phase packet. The many-body density distribution is expressed in a Hartree approximation as a product of distributions for each particle.[7,17] Equations of motion for the density distribution are derived for both constant energy and constant temperature dynamics and exact results are obtained for the time evolution in the free particle and harmonic potentials.

We demonstrate the general applicability of the Gaussian phase packet dynamics method through two applications. The first involves the calculation of equilibrium thermodynamic averages for a Lennard-Jones cluster and fluid using Gaussian phase packets. We find that the constant

[a]Present address: Department of Chemistry, Wellesley College, Wellesley, MA 02181-8201.

 0021-9606/93/99(5)/4024/12/$6.00

energy Gaussian phase packet dynamics provides a reasonable description of the fluid structure and thermodynamics at moderate to low temperatures. In the second application, we develop a global optimization algorithm based on simulated annealing of the phase space density distribution. The annealing algorithm is applied to find the global energy minimum for a series of Lennard-Jones clusters and found to be significantly better than annealing schemes employing molecular dynamics simulation of point particles.

II. METHODS

In this section, we present equations of motion for constant energy and constant temperature dynamics based on approximate solution of the Liouville equation using a Gaussian phase packet representation of the density distribution. We begin with a discussion of the equations for a single particle moving in an external potential and then generalize the treatment to many-body systems. The equations of motion can be used, as can molecular dynamics simulation, to examine the nonequilibrium relaxation process or to perform equilibrium averages. We discuss the relationship between molecular dynamics, the ergodic hypothesis, and the GPP dynamics to make clear the connection between time averages over GPP trajectories and equilibrium thermodynamic averages for the system. Finally, we provide a measure of the rate of kinetic energy equipartitioning through a generalization of the ergodic measure for GPPs.

A. Background

The average of any observable property over an ensemble of systems may be conveniently expressed as an average of the property $A(r,p)$ over all phase space weighted by the density distribution $\rho(r,p,t)$,[18]

$$\langle A\rangle = \int d^d r \int d^d p\, \rho(r,p,t) A(r,p). \tag{1}$$

Calculating $\rho(r,p,t)$ is the central task of classical statistical mechanics. The time evolution of $\rho(r,p,t)$ is described by the Liouville equation[8,19]

$$\frac{\partial}{\partial t}\rho(r,p,t) = -L_0 \rho(r,p,t), \tag{2}$$

where L_0 is the Liouville operator

$$L_0 = \frac{p}{m}\cdot\frac{\partial}{\partial r} + F(r)\cdot\frac{\partial}{\partial p} \tag{3}$$

and where $F(r)$ is the force and m is the mass. $F(r)$, r, and p are d-dimensional vectors.

While a general solution of Eq. (2) is forbidding for many-body systems with nonlinear interaction potentials, it is possible to replace the Liouville equation for $\rho(r,p,t)$ with a set of equations for the moments of the distribution. The equations of motion for the average position and momentum are

$$\frac{\partial\langle r\rangle}{\partial t} = \frac{\langle p\rangle}{m} \quad \frac{\partial\langle p\rangle}{\partial t} = \langle F\rangle \tag{4}$$

and for the higher-order moments of position and momentum

$$\frac{\partial M_{n,k}}{\partial t} = \frac{n}{m} M_{n-1,k+1} + k W_{n,k-1}. \tag{5}$$

The moments of the distribution are defined as

$$M_{n,k} = \langle (r-r_0)^n (p-p_0)^k \rangle, \tag{6}$$

$$W_{n,k} = \langle (r-r_0)^n (p-p_0)^k (F-F_0)\rangle, \tag{7}$$

where $r_0 = \langle r\rangle$, $p_0 = \langle p\rangle$, and $F_0 = \langle F(r)\rangle$. This hierarchy of equations describes the time evolution of $\rho(r,p,t)$ exactly and is independent of the basis set employed. A detailed derivation of Eq. (5) is given in Appendix A.

B. Gaussian phase packets at constant energy

As a first approximation, we represent the phase space density distribution function for each degree of freedom in d dimensions as a single spherically symmetric GPP

$$\rho(r,p,t) = \left(\frac{\sqrt{1-\alpha^2}}{2\pi\sigma_a\sigma_b}\right)^d \exp\left[-\frac{1}{2}\left(\frac{r-r_0}{\sigma_a}\right)^2 - \frac{1}{2}\left(\frac{p-p_0}{\sigma_b}\right)^2 - \alpha\left(\frac{r-r_0}{\sigma_a}\right)\left(\frac{p-p_0}{\sigma_b}\right)\right]. \tag{8}$$

In our notation, we neglect the explicit time dependence of r_0, p_0, σ_a, σ_b, and α. It is straightforward to derive equations of motion for each Gaussian using Eq. (5). The time dependences of the GPP parameters is completely specified by the time evolution of the average position $\langle r\rangle$ and momentum $\langle p\rangle$ and the second-order moments in d dimensions

$$M_{2,0} = \frac{d\sigma_a^2}{(1-\alpha^2)} = -\frac{\sigma_a}{\alpha\sigma_b} M_{1,1} = \frac{\sigma_a^2}{\sigma_b^2} M_{0,2}. \tag{9}$$

A useful identity is

$$W_{0,1} = -\frac{\alpha\sigma_b}{\sigma_a} W_{1,0} = -\frac{1}{d} M_{1,1} \nabla_{r_0}^2 \langle V\rangle. \tag{10}$$

The resulting first-order equations of motion for the Gaussian phase packet are

$$\dot r_0 = \frac{p_0}{m}, \quad \dot p_0 = -\nabla_{r_0}\langle V\rangle, \quad \dot M_{2,0} = \frac{2}{m} M_{1,1},$$
$$\dot M_{1,1} = \frac{1}{m} M_{0,2} - \frac{1}{d} M_{2,0} \nabla_{r_0}^2 \langle V\rangle, \quad \dot M_{0,2} = -\frac{2}{d} M_{1,1} \nabla_{r_0}^2 \langle V\rangle. \tag{11}$$

This set of $(2d+3)$ first-order equations describing the time evolution of the density distribution for each particle is equivalent to that of the analogous quantum system.[13] These equations are identical to the variationally optimized equations of motion resulting from application of the Dirac–Frenkel variational principle[20] adapted to the Liouville equation. Note that $\langle V\rangle$ is the bare potential energy averaged over the phase space distribution

$$\langle V\rangle \equiv \int dr \int dp\, \rho(r,p) V(r). \tag{12}$$

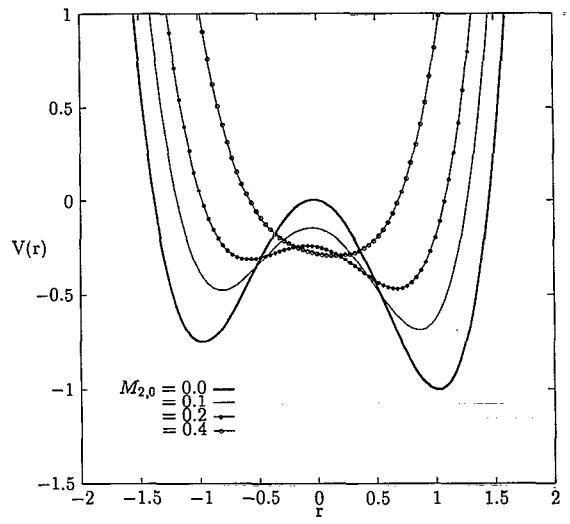

FIG. 1. The effective potential defined by Eq. (12) is plotted for an asymmetric double well for a series of squared widths $M_{2,0}$. The bare potential used in molecular dynamics corresponds to $M_{2,0}=0$. The units are arbitrary. The potential is approximately what would be seen by a Lennard-Jones atom moving along r between two Lennard-Jones atoms centered at $r=\pm 2$.

Averaging over the density distribution $\rho(r,p)$ effectively coarse grains the potential surface. In Fig. 1, we show how the effective potential is smoothed as the width of the density distribution increases.[21]

We make five observations concerning the equations of motion for the Gaussian phase packet. (1) In the limit that $M_{2,0}$ goes to zero, the equations of motion of the GPP centers reduce to those of standard Newtonian molecular dynamics where $\rho(r,p,t)=\delta(r-r_0)\delta(p-p_0)$. (2) The centers of the Gaussian phase packet respond to the gradient of the effective potential $\langle V\rangle$, while the widths change as the Laplacian of the effective potential. (3) The single GPP provides an incomplete description of the phase space density distribution; however, the total energy is conserved. (4) We found the moment equations to be of stiffness comparable to Newton's equations of motion. (5) In highly anisotropic spaces, it would be helpful to employ ellipsoidal Gaussians by replacing the scalar α and σ's with $d\times d$ matrices.

C. Gaussian phase packets at constant temperature

To apply the constant temperature constraint, we appeal to Gauss' principle[22] and write the generalized Liouvillian

$$L=\frac{p}{m}\cdot\frac{\partial}{\partial r}+F(r)\cdot\frac{\partial}{\partial p}-\gamma\frac{\partial}{\partial p}\cdot p=L_0-\gamma\frac{\partial}{\partial p}\cdot p, \tag{13}$$

where γ is determined by the external constraint equation

$$\frac{\partial\langle p^2\rangle}{\partial t}=0, \tag{14}$$

which guarantees that the temperature remain constant at every instant in time.

Using the Liouville equation (in the Heisenberg representation), we find equations of motion for the average position and momentum

$$\frac{\partial\langle r\rangle}{\partial t}=\frac{\langle p\rangle}{m}, \tag{15}$$

$$\frac{\partial\langle p\rangle}{\partial t}=\langle F\rangle-\gamma\langle p\rangle, \tag{16}$$

and for the higher-order moments of position and momentum

$$\frac{\partial M_{n,k}}{\partial t}=\frac{n}{m}M_{n-1,k+1}+k(W_{n,k-1}-\gamma M_{n,k}). \tag{17}$$

The above equations are exact and completely general. For the Gaussian phase packet, the time evolution of the first- and second-order moments is given by

$$\dot r_0=\frac{p_0}{m},\quad \dot p_0=-\nabla_{r_0}\langle V\rangle-\gamma p_0,\quad \dot M_{2,0}=\frac{2}{m}M_{1,1},$$

$$\dot M_{1,1}=\frac{1}{m}M_{0,2}-\frac{1}{d}M_{2,0}\nabla^2_{r_0}\langle V\rangle-\gamma M_{1,1}, \tag{18}$$

$$\dot M_{0,2}=-\frac{2}{d}M_{1,1}\nabla^2_{r_0}\langle V\rangle-2\gamma M_{0,2}.$$

The temperature constraint equation, which determines the value of γ, is

$$\gamma=\frac{p_0\cdot F_0+W_{0,1}}{p_0^2+M_{0,2}}, \tag{19}$$

where we have used the fact that $\langle p^2\rangle=p_0^2+M_{0,2}$. Note that in general

$$m\ddot r_0=-\nabla_{r_0}\langle V\rangle-\gamma p_0 \tag{20}$$

for the Gaussian center r_0 moving in a coarse-grained effective potential. In the limit that $M_{2,0}=0$, the equations of motion reduce to the constant temperature algorithm of Evans and Hoover for classical point particles.

D. Many-body systems

In the previous sections, we derived equations of motion for $\rho(r,p,t)$ of a single particle in d dimensions. When many particles are introduced, the density distribution may in the first approximation be written as a product of the density distributions of the N individual particles

$$\rho(r^N,p^N,t)=\prod_{k=1}^{N}\rho^{(k)}(r^{(k)},p^{(k)},t). \tag{21}$$

This is in the spirit of the Hartree approximation of quantum mechanics.

The equations of motion derived in the previous section can be used for each particle, where $F(r)$ is taken to be the integral of the force weighted by the total density distribution integrated over all other particles; i.e., $F(r)$ is averaged over the positions of all the other particles—a

mean field force.[23] For a pairwise additive potential, the force on the ith particle due to all other particles can be expressed

$$\langle F(r^{(i)})\rangle = \sum_{k\neq i} \int dr^{(k)} \int dp^{(k)} \rho^{(k)}(r^{(k)},p^{(k)}) \times F(|r^{(i)}-r^{(k)}|). \quad (22)$$

Similarly, the potential energy is a sum over the individual pair interaction energies

$$\langle V\rangle = \sum_{i>j=1}^{N} \int dr^{N} \int dp^{N} \rho(r^{N},p^{N}) V(|r^{(i)}-r^{(j)}|) = \sum_{i>j=1}^{N} \int dr^{(i)} \int dp^{(i)} \int dr^{(j)} \int dp^{(j)} \times \rho^{(i)}(r^{(i)},p^{(i)}) \rho^{(j)}(r^{(j)},p^{(j)}) V(|r^{(i)}-r^{(j)}|). \quad (23)$$

When the potential is not pairwise additive, the density distribution functions for two or more particle correlations must be used. For a many-body system, the temperature constraint equation for the N-body system [generalized from Eq. (19)] leads to

$$\gamma = \sum_{k=1}^{N} (p_0^{(k)} \cdot F_0^{(k)} + W_{0,1}^{(k)}) \Big/ \sum_{k=1}^{N} (p_0^{(k)2} + M_{0,2}^{(k)}), \quad (24)$$

where we write the sum over all N particles forming the system.

In our study of many particle systems, we will define the structure in terms of radial distribution functions for the probability of finding two particles some radial distance r apart. For the case of a pair of Gaussian phase packets, this probability is

$$G(r) = \left(\frac{\zeta}{\pi}\right)^{1/2} \frac{r}{r_{12}} \{\exp[-\zeta(r-r_{12})^2] - \exp[-\zeta(r+r_{12})^2]\}, \quad (25)$$

where $\zeta = d/[2(M_{2,0}^{(1)} + M_{2,0}^{(2)})]$ and r_{12} is the distance between the distribution centers of particles 1 and 2. In the limit that the squared widths $M_{2,0}$ of the Gaussian phase packets go to zero, $G(r) = \delta(r-r_{12})$ as for the case of point particles in standard molecular dynamics. In the calculation of the pair correlation function using GPP dynamics, one bins the continuous function $G(r)$ over a range of r rather than counting as in the case of discrete particles. A detailed derivation of Eq. (25) is presented in Appendix B.

Note that when strong correlations exist between degrees of freedom, the density distribution may be expanded in coordinates as close as possible to the local, or if possible, normal, modes of the system. For example, when two particles are connected by a chemical bond, the bond itself can be taken as a degree of freedom rather than simply the coordinates of the individual particles.

E. Taking equilibrium averages

The validity of conventional molecular dynamics (MD) simulation rests on the assumption that the ergodic hypothesis which equates time and equilibrium ensemble average properties is valid. In this section, we establish the connection between equilibrium time averages taken over MD and GPP trajectories.

A MD trajectory of a single phase point in a d- dimensional space of N particles is defined in terms of a $2dN$-dimensional vector for the position and momentum $[r_0^N(t), p_0^N(t)]$. The classical density distribution for a MD trajectory is

$$\rho_{\mathrm{MD}}(r^N,p^N,t) = \delta[r^N - r_0^N(t)]\delta[p^N - p_0^N(t)]. \quad (26)$$

Inserting $\rho_{\mathrm{MD}}(r^N,p^N,t)$ into the Liouville equation $\dot{\rho} = -L_0\rho$ leads to Newton's equations of motion for the positions and momenta $[r_0^N(t), p_0^N(t)]$ of the N particle system. The ergodic hypothesis equating the equilibrium time and phase space averages for a property $A(r^N,p^N)$ is

$$\lim_{T\to\infty} \frac{1}{T} \int_0^T A[r_0^N(t), p_0^N(t)]\,dt = \int dr^N dp^N A(r^N,p^N) \rho_{\mathrm{eq}}(r^N,p^N), \quad (27)$$

where $H(r^N,p^N)$ is the system Hamiltonian, $\rho_{\mathrm{eq}}(r^N,p^N) = \exp(-\beta H)/Q, Q(\beta) = \int dr\,dp \exp(-\beta H)$ is the equilibrium canonical partition function, and

$$A[r_0^N(t), p_0^N(t)] = \int dr^N dp^N A(r^N,p^N) \rho_{\mathrm{MD}}(r^N,p^N,t). \quad (28)$$

Time averaging over a single long MD trajectory has been shown to be an inefficient way to calculate thermodynamic properties for large biological molecules.[4] An alternative simulation protocol, running many shorter MD trajectories with independent initial conditions, has been shown to generate more effective sampling for certain systems.[24] For the case of biomolecules or glasses, effective sampling of phase space with a single trajectory can require activated transitions over significant energy barriers. By running many quasi-independent trajectories, it is possible to sample independent regions of phase space, which may be separated by significant energy barriers without waiting exponentially long times for an activated barrier crossing from one region to another. As such, sampling with many shorter quasi-independent trajectories might *exponentially* increase the rate of convergence in thermodynamic averages over similar calculations employing a single long MD trajectory.

Now let us assume we have a bundle of M independent trajectories which we want to integrate concurrently. This set of independent MD trajectories can be represented by a single density distribution trajectory.[17] The density distribution for the trajectory bundle is

$$\rho_{\mathrm{bundle}}(r,p,t) = \frac{1}{M} \sum_{k=1}^{M} \delta[r - r_k(t)]\delta[p - p_k(t)] \quad (29)$$

and the ergodic hypothesis, which is valid for each of the individual trajectories, will be valid for the sum over the set of M trajectories

$$\lim_{T\to\infty}\frac{1}{T}\int_0^T\left\{\frac{1}{M}\sum_{k=1}^{M}A[r_k(t),p_k(t)]\right\}dt$$

$$=\int dr\,dp\,A(r,p)\rho_{\rm eq}(r,p). \tag{30}$$

Our goal is to develop a simulation method where a continuous distribution can substitute for the bundle of many individual trajectories. This is the same as finding a proper representation for the phase space density distribution function whose time evolution is described by the classical Liouville equation. By making an approximation to the exact density distribution, we hope to gain enhanced sampling over standard MD, but with a savings in computational effort as compared with the trajectory bundle method. This is in the spirit of the locally enhanced sampling (LES) algorithm of Elber and co-workers.[7]

In our work on Gaussian phase packets, we are making the approximation that the distribution $\rho_{\rm bundle}(r,p,t)$ for the bundle of M trajectories may be approximated by a continuous Gaussian density, i.e.,

$$\rho_{\rm bundle}(r,p,t)=\frac{1}{M}\sum_{k=1}^{M}\delta[r-r_k(t)]\delta[p-p_k(t)]$$

$$\simeq\rho_{\rm GPP}(r,p,t). \tag{31}$$

Combining the result from Eq. (30) and Eq. (31) leads to

$$\lim_{T\to\infty}\frac{1}{T}\int_0^T\left[\int dr\,dp\,A(r,p)\rho_{\rm GPP}(r,p,t)\right]dt$$

$$\simeq\int dr\,dp\,A(r,p)\rho_{\rm eq}(r,p). \tag{32}$$

When Eq. (31) is a reasonable approximation, we can expect that the time average over our GPP trajectory will be a good estimate of the equilibrium thermodynamic average for the system.

F. Generalized kinetic energy fluctuation metric

It is of interest to compare the efficiency of phase space sampling between molecular and GPP dynamics. The rate of kinetic energy equipartitioning may be compared using a generalization of the kinetic energy fluctuation metric.[4,25] The time average of the kinetic energy is

$$f_j(t)=\frac{1}{2mt}\int_0^t d\tau\,p_j^2(\tau) \tag{33}$$

in terms of the momentum p_j of the jth particle of mass m. The average of $f_j(t)$ over all N particles is $\bar{f}(t)$. The kinetic energy fluctuation metric is defined

$$\Omega(t)=\frac{1}{N}\sum_{j=1}^{N}[f_j(t)-\bar{f}(t)]^2. \tag{34}$$

For ergodic systems, at long times the fluctuation metric decays to zero as $\Omega(0)/\Omega(t)=D_{\rm KE}t$, where $D_{\rm KE}$ is a generalized diffusion coefficient defining the rate of kinetic energy equipartitioning.[25]

A system of Gaussian phase packets represents an infinite ensemble of phase points. Each phase point represents a realization of the full system. We would like to generalize the kinetic energy fluctuation metric defined above for a single phase point to an ensemble of phase points.

Suppose we have an ensemble of M representations of our N particle system. The time averaged kinetic energy of the jth particle in the kth system of the ensemble is $f_{j,k}(t)$. By averaging over the ensemble, we can define the time and ensemble averaged kinetic energy for the jth particle as

$$\hat{f}_j(t)=\frac{1}{M}\sum_{k=1}^{M}f_{j,k}(t). \tag{35}$$

Furthermore, the average of $f_{j,k}(t)$ over all N particles is $\hat{\bar{f}}(t)$.

The generalization of the kinetic energy fluctuation metric for an ensemble of systems is

$$\hat{\Omega}(t)=\frac{1}{N}\sum_{j=1}^{N}[\hat{f}_j(t)-\hat{\bar{f}}(t)]^2. \tag{36}$$

If the system is ergodic, as the number M of systems in the ensemble is increased, the individual particle averages $\hat{f}_j(t)$ will converge to the system average $\hat{\bar{f}}(t)$ leading to convergence in $\hat{\Omega}(t)$. In fact, as $M\to\infty$ and the density distribution approaches the equilibrium ensemble, the metric $\hat{\Omega}(t)\to 0$ for any t, regardless of the system size N.

To compare the rate of energy equipartitioning in GPP simulations with molecular dynamics, we employ the generalization of the kinetic energy fluctuation metric. For GPP simulations, the ensemble average above corresponds to integrating over the Gaussian phase packet. Therefore, for each particle, we use $\hat{f}_j(t)=\langle p^2/2m\rangle=(p_0^{(j)2}+M_{0,2}^{(j)})/2m$ in the expression for the time and ensemble averaged kinetic energy. Furthermore, we note that the initial value of the generalized fluctuation metric is $\Omega(0)=3(k_BT)^2/2$ when the number of systems in the ensemble $M=1$. Following the discussion above, when $M>1$, we expect $\hat{\Omega}(0)<\Omega(0)$. To account for the increased convergence in the metric, even at $t=0$, we employ the normalized metric $\Omega(0)/\hat{\Omega}(t)$. This normalized metric will initially be unity for a single system of point particles (molecular dynamics) and greater than unity for the GPP system.

III. APPLICATIONS OF GAUSSIAN PHASE PACKET DYNAMICS

We briefly discuss the results for free particle and harmonic potentials. Results of equilibrium thermodynamic averages taken for a 55 atom cluster and 256 atom fluid of Lennard-Jones atoms represented by Gaussian phase packets in the Hartree approximation are presented and compared with data derived from "exact" molecular dynamics simulations. Finally we present results for global energy minimization of a series of Lennard-Jones clusters using simulated annealing of GPPs.

A. The free particle and harmonic oscillator

For the free particle, $V(r)=$constant, and

$$\frac{\partial M_{n,k}}{\partial t}=\frac{n}{m}M_{n-1,k+1}. \tag{37}$$

This result is independent of the shape of the distribution. Note that only moments of the same order $n+k$ are coupled.

Due to the fact that the center of the distribution is moving with constant momentum and the moment $M_{0,2}$ is independent of time, the instantaneous ideal gas temperature

$$T=\frac{1}{mdk_B}(p_0^2+M_{0,2}) \tag{38}$$

is constant. We note that if $\alpha=0$ for all time in Eq. (8), there is insufficient flexibility in the Gaussian approximation to $\rho(r,p)$ to provide the exact solution for the time evolution of the density distribution of the free particle.

The general dynamics for the density distribution in a harmonic potential $V(r)=\kappa r^2/2$ is

$$\frac{\partial M_{n,k}}{\partial t}=\frac{n}{m}M_{n-1,k+1}-k\kappa M_{n+1,k-1}. \tag{39}$$

This result is exact for any initial phase packet. As for the free particle, only moments of the same order $n+k$ are coupled. We note that the second moments oscillate in time with twice the frequency of the distribution centers, as is found for the quantum oscillator.[26]

B. Equilibrium averages for a Lennard-Jones cluster and fluid

A two-term sum of Gaussians provides a reasonably accurate representation of the Lennard-Jones potential. For the case of Gaussian phase packets, we need evaluate only the first and second derivatives of the effective potential $\langle V\rangle$. For a single Gaussian potential $V(r)=\exp[-\lambda(r-r_m)^2/2]$, the results are

$$\begin{aligned}\langle V\rangle&=\left(\frac{\hat{\lambda}}{\lambda}\right)^{d/2}\exp\left[-\frac{1}{2}\hat{\lambda}(r_0-r_m)^2\right],\\ \nabla_{r_0}\langle V\rangle&=-\hat{\lambda}(r_0-r_m)\langle V\rangle,\\ \nabla_{r_0}^2\langle V\rangle&=\hat{\lambda}[\hat{\lambda}(r_0-r_m)^2-d]\langle V\rangle,\end{aligned} \tag{40}$$

where $\hat{\lambda}=\lambda/(1+\lambda M_{2,0}/d)$. The parameters for the two Gaussian fit to the Lennard-Jones potential of the form $V(r)=\Sigma_k a_k e^{-b_k r^2}$ given in Lennard-Jones reduced units are $a_1=14\,487.1$, $b_1=9.051\,48$ and $a_2=-5.553\,38$, $b_2=1.225\,36$ (similar to the parameterization in Ref. 27). We use this approximate two Gaussian decomposition of the potential for both the GPP and poin<t particle molecular dynamics simulations.

We simulated a cluster and fluid of Lennard-Jones atoms where the density distribution of each atom was represented as a Gaussian phase packet and the many-body distribution was approximated as a Hartree product. The equations of motion for both molecular dynamics and GPP dynamics were integrated using the fourth order Gear algorithm with a time step of 0.002 Lennard-Jones time units.[1] The total energy was constrained to give approximately the same average temperature for each system. Each system was equilibrated by warming over ten time units to the desired temperature, followed by ten time units of constant temperature dynamics, and ten time units of constant energy dynamics; averaging was performed over 50 time units in computing structure, thermodynamics, and the kinetic energy fluctuation metric. Equilibration for the Gaussian phase packets was performed using the constant temperature version of our GPP dynamics algorithm described above. The constant temperature molecular dynamics was performed using the algorithm derived by Hoover and Evans.[22] There was no significant evaporation during the cluster simulation. For the dynamics of the Lennard-Jones systems, total energy was conserved to better than 10^{-4} for both standard molecular dynamics and GPP dynamics.

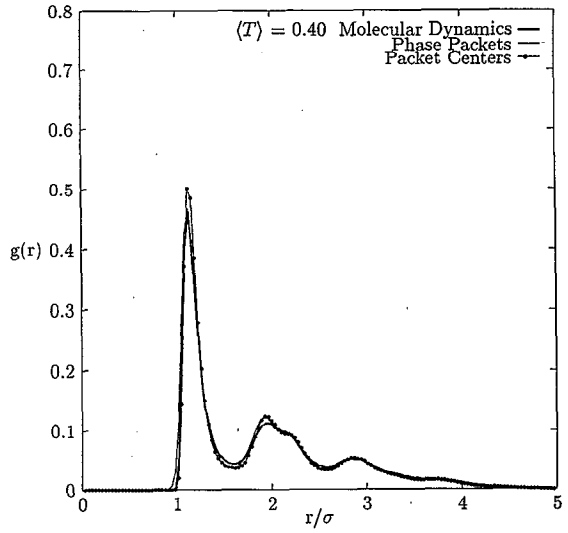

FIG. 2. The radial distribution functions for the 55 atom Lennard-Jones cluster derived from Gaussian phase packet dynamics and standard molecular dynamics at the average reduced temperature $\langle T\rangle=0.40$. Shown for comparison is the radial distribution function of the Gaussian packet centers. Each distribution function is normalized to the total particle number.

Shown in Fig. 2 are the radial distribution functions for a 55 atom cluster at an average reduced temperature of $\langle T\rangle=0.40$ derived from Newtonian molecular dynamics simulation of point particles and GPP dynamics. At this low temperature, there is close agreement between the point particle and Gaussian phase packet results. The radial distribution functions show glass-like structure in the split second peak for both point particles and, more distinctly, Gaussian phase packets. For comparison, we also display the pair distribution function of the Gaussian centers. There is little difference between the distribution of the centers and the full distribution averaged over the width of the Gaussian phase packets, indicating that the packets are on average quite narrow.

TABLE I. Results from Gaussian phase packet (GPP) dynamics and molecular dynamics (MD) simulations of a 55 atom cluster and 256 atom fluid for the average potential energy $\langle V\rangle$ and temperature $\langle T\rangle$ at a fixed total energy E and density $\hat{\rho}$. The time averaged second moments $M_{2,0}$, $M_{1,1}$, and $M_{0,2}$ are given for the GPP simulations.

N	$\hat{\rho}$	$\langle T\rangle$	Method	E	$\langle V\rangle$	$\sqrt{M_{2,0}}$	$M_{1,1}\times 10^6$	$M_{0,2}$
55	Cluster	0.40	MD	−3.12	−3.72			
		0.42	GPP	−3.12	−3.75	0.0682	112	0.356
256	0.844	0.70	MD	−4.52	−5.56			
		0.71	GPP	−4.53	−5.59	0.0482	46.6	0.616
256	0.65	1.25	MD	−2.10	−3.97			
		1.24	GPP	−2.11	−3.96	0.121	40.0	2.37
		2.01	MD	−0.57	−3.61			
		1.99	GPP	−0.57	−3.60	0.132	−73.5	3.84
256	0.75	1.26	MD	−2.65	−4.55			
		1.25	GPP	−2.70	−4.60	0.100	35.2	2.29
		2.00	MD	−1.09	−4.07			
		2.00	GPP	−1.11	−4.10	0.115	−52.8	3.95
256	0.85	1.23	MD	−3.29	−5.07			
		1.24	GPP	−3.31	−5.10	0.090	0.38	2.52
		1.98	MD	−1.47	−4.39			
		2.01	GPP	−1.50	−4.42	0.112	−30.4	4.31

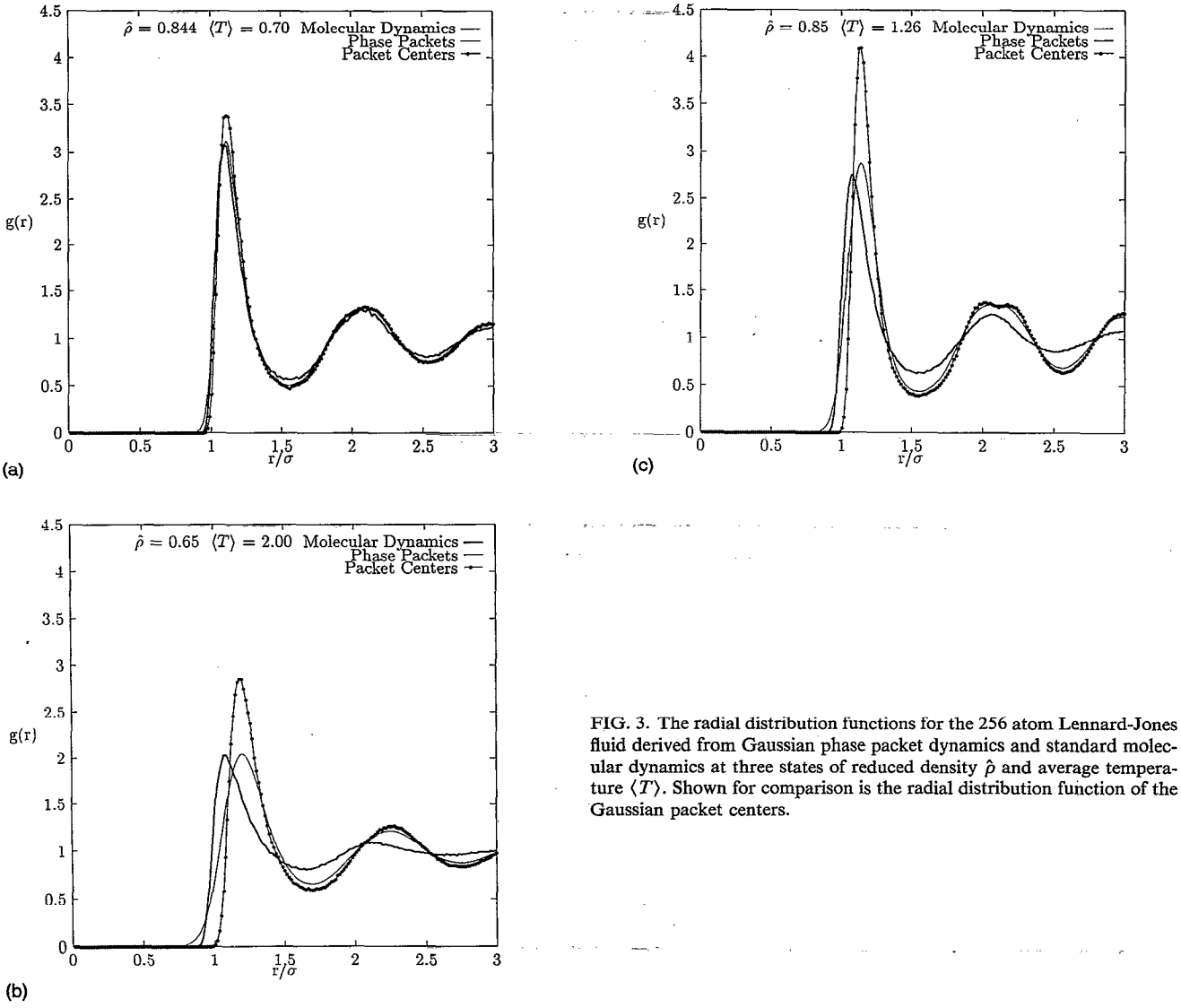

FIG. 3. The radial distribution functions for the 256 atom Lennard-Jones fluid derived from Gaussian phase packet dynamics and standard molecular dynamics at three states of reduced density $\hat{\rho}$ and average temperature $\langle T\rangle$. Shown for comparison is the radial distribution function of the Gaussian packet centers.

Listed in Table I are the time-averaged potential energy and temperature of the 55 atom cluster for molecular dynamics and GPP dynamics. The cluster results are very close to the exact results derived from molecular dynamics simulation. For this state point, the Gaussian packets are narrow, with an average width $\sqrt{M_{2,0}} = 0.068$, and the GPP effective potential seen by the centers differs little from the bare Lennard-Jones potential (see below).

Figure 3 displays the radial distribution functions for the 256 atom Lennard-Jones fluid at three states of reduced density $\hat{\rho}$ and average temperature $\langle T \rangle$. The fluid simulations employed periodic boundary conditions with a potential cutoff of 3.5σ at the lowest density and 3.0σ at higher density. Near the triple point ($\hat{\rho}=0.844$ and $\langle T \rangle = 0.70$), the average fluid structure for the Gaussian phase packets is close to the exact result of the molecular dynamics trajectory. At higher temperature ($\langle T \rangle = 1.25$ and 2.00) and all densities examined, the Gaussian phase packet distribution function has a first peak which is similar in height, shifted out, penetrating to smaller separations, and slightly broadened relative to the molecular dynamics result. The distribution of Gaussian packet centers shows a higher first peak than the molecular dynamics results or the average structure over the full density distribution. In addition, there are more pronounced oscillations in the GPP structure in the second and third solvation shells. This heightened structure indicates a greater tendency of the broadened spherical Gaussian packets to pack in an orderly fashion.

The average widths of the Gaussian phase packets are presented along with the thermodynamic results in Table I. The time averaged values of $M_{1,1}$ are small, indicating the coupling between position and momentum time averages to near zero, as it must if the time average of the density distribution is to equal the equilibrium density distribution. The average squared width in momentum $M_{0,2}$ accounts for approximately one-third of the temperature for the cluster and the fluid near the triple point; the remaining contribution to the temperature is made by the time average of the mean-square momentum of the packet centers p_0^2. At all densities, for average temperatures $\langle T \rangle = 1.25$ and 2.00, $M_{0,2}$ accounts for roughly two-thirds of the temperature.

The averaged width in position space $\sqrt{M_{2,0}}$ for the state near the triple point is similar to that found for the low temperature cluster. At higher temperature, the width is slightly larger. In Fig. 4, we show the effective potential for the packet centers, defined by Eq. (12), for fixed widths representing the average squared width $M_{2,0}$ from the three fluid simulations represented in Fig. 3. As the packet width increases, the effective potential minimum shifts outward. The position of this minimum is strongly correlated (within 0.02σ) with the position of the first peak in the radial distribution function for the corresponding state.

The thermodynamic results summarized in Table I show the average potential energy for the GPP system agrees with the result of the point particle molecular dynamics. While the approximations employed to represent the density distribution assume spherically symmetric

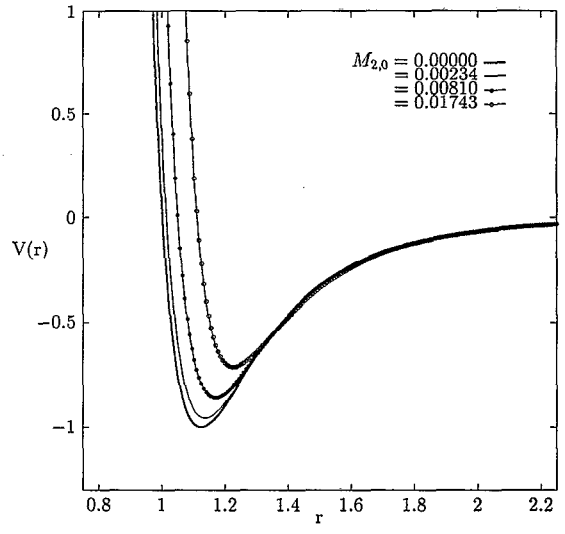

FIG. 4. The effective potential defined by Eq. (12) is plotted for the two Gaussian fit to the Lennard-Jones potential for a series of widths $\sqrt{M_{2,0}}$. The widths are derived from the Gaussian phase packet simulations and correspond to the three radial distribution functions in Fig. 3. The bare potential used in molecular dynamics corresponds to $M_{2,0}=0$.

Gaussian packets and ignore correlation in the Hartree approximation, the result of GPP dynamics is within a few percent of the exact results at all state points examined.

A comparison between the rate of kinetic energy equipartitioning using Gaussian phase packet and molecular dynamics simulation is summarized in Table II. The rate of kinetic energy equipartitioning is faster for GPP dynamics when compared with standard molecular dynamics simulation for all six state points examined. In Fig. 5, we show the inverse normalized generalized kinetic energy metric $\Omega(0)/\hat{\Omega}(t)$ for both the GPP dynamics and molecular dynamics. The difference in initial value of $\Omega(0)/\hat{\Omega}(t)$ between the GPP and molecular dynamics methods, which is typically a factor of 3–5, indicates that before any dynamical averaging has taken place, there is significant convergence in the GPP system due to the distribution of momenta. The rate of equipartitioning D_{KE} is approximately three to four times larger for the GPP dynamics of all fluid states examined (see Table II).

TABLE II. The kinetic energy diffusion constant D_{KE} calculated from the generalized kinetic energy fluctuation metric for the 256 atom Lennard-Jones fluid for Gaussian phase packets, normalized by the value calculated for standard molecular dynamics, at six state points of reduced density $\hat{\rho}$ and average temperature $\langle T \rangle$. The initial value $\Omega(0)/\hat{\Omega}(0)$ for GPP dynamics is listed in parentheses.

	$\hat{\rho}$		
$\langle T \rangle$	0.65	0.75	0.85
1.25	3.24	2.75	2.23
	(3.83)	(4.01)	(5.08)
2.00	3.80	2.96	2.83
	(3.99)	(3.75)	(5.05)

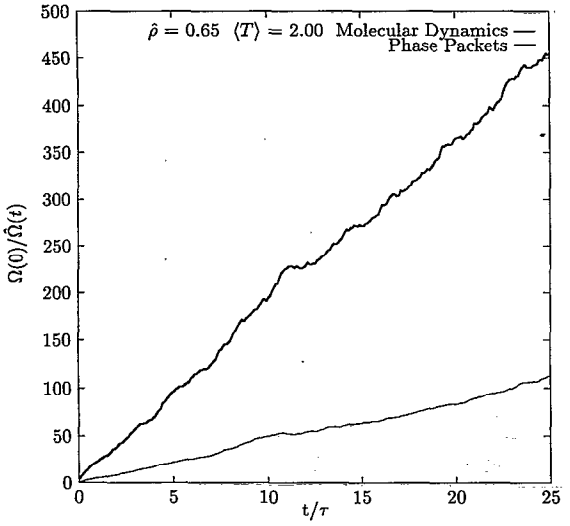

FIG. 5. The inverse normalized generalized kinetic energy metric $\Omega(0)/\hat{\Omega}(t)$ defined by Eq. (36) for the state point $\hat{\rho}=0.65$ and $\langle T\rangle=2.00$.

C. Global potential energy minimization

Recently, substantial progress has been made on the problem of global energy minimization for molecular systems. Much of this work has been focused on the protein folding problem where it is believed that the global energy minimum of a compact protein may be a good estimate of the protein's folded state conformation.[28–33] In this section, we present a method for global potential energy minimization based on the simulated annealing[34] of Gaussian phase packets. The annealing algorithm, developed from the constant temperature algorithm described above, was used to find global energy minimum structures for a series of Lennard-Jones n-mer clusters ranging from $n=8$–19. The results are shown in Table III.

In our previous discussion of the constant temperature algorithm, the system temperature was taken to be a constant, i.e., $\partial T/\partial t=0$. For our simulated annealing algorithm, we adopt an exponential cooling rate $T(t)=T(0)\exp(-\eta t)$. The constraint equation which determines γ is $\partial T/\partial t=-\eta T$. The annealing dynamics is defined by Eq. (18) combined with the generalization of Eq. (24) for exponential cooling

$$\gamma=\frac{\eta}{2}+\sum_{k=1}^{N}(p_0^{(k)}\cdot F_0^{(k)}+W_{0,1}^{(k)})\Big/\sum_{k=1}^{N}(p_0^{(k)2}+M_{0,2}^{(k)}). \tag{41}$$

The relaxation rate η will control how fast the temperature is reduced in the annealing dynamics. The annealing dynamics algorithm was employed in the following general protocol for global optimization and energy minimization:

(1) The initial configuration should be the best guess at the global minimum structure. In this work, we randomly chose initial configurations from a high temperature Lennard-Jones cluster simulation.

(2) The equations of motion (18) and (41) were integrated using the Bulirsch–Stoer method with an internal relative error tolerance of 10^{-8}.

(3) The initial moments of the phase packet should be chosen large. In this work, we chose the initial values of p_0 and α to be zero. The moments were chosen to be in the range $M_{2,0}\in(0.75,3.0)$, $M_{0,2}\in(4.5,7.5)$, $T(0)\in(1.5,2.5)$, and $M_{1,1}=0$ in Lennard-Jones reduced units. For the GPP, the annealing rate is $\eta=0.2$.

(4) The annealing trajectory was followed until the final temperature $T(t=100)=T(0)e^{-10}$. At this point, the conjugate gradient algorithm with the exact Lennard-Jones potential was used to refine the energy of the minimum.

(5) During the simulation, a relatively wide boundary potential of the form

$$V_{\text{conf}}=(r/r_{\text{wall}})^{20}, \tag{42}$$

where $r_{\text{wall}}=3$–4 was fixed around the cluster to prevent dissociation at high temperature.

For comparison, we also ran the pure MD annealing dynamics using the same initial conditions and the constant temperature algorithm of Evans and Hoover, where γ is modified to follow an exponential cooling rate [essentially Eq. (41) for $M_{0,2}=W_{0,1}=0$]. We found that the conventional MD simulated annealing was not able to locate the same minimum structure for any cluster size using $\eta=0.2$. The global minimum was found using the point particle MD simulated annealing only when the cooling rate was substantially reduced. We investigated the maximum cooling rate for simulated annealing using both GPP and MD. Either method can find the global minimum for clusters with $n=8$, 13, and 19. We found the typical fast cooling rate for GPP to be $\eta=0.2$ and the typical fast cooling rate for pure MD to be $\eta=0.005$. The GPP annealing rate is 40 times faster than for simulated annealing with standard MD. One possible explanation for the difference in cooling rates is the faster rate of potential energy relaxation for the GPP. When the temperature is decreased during the annealing run, the potential energy must relax or the simulation should effectively sample the phase space. At high temperatures, the GPPs are delocalized and able

TABLE III. Global energy minimization results from Gaussian phase packet simulated annealing simulations for Lennard-Jones n-mer clusters. Energies are given in Lennard-Jones reduced units.

No. of atoms	No. of minima[a]	Energy[b,c]	GPP ($\eta=0.2$)	MD ($\eta=0.2$)	MD ($\eta=0.005$)
8	8	−19.822	−19.822	−18.830	−19.822
9	18	−24.113	−24.113		
10	57	−28.420	−28.420		
11	145	−32.765	−32.765		
12	366	−37.967	−37.967		
13	988	−44.327	−44.327	−40.655	−44.327
14	2 617	−47.845	−47.845		
15	6 923	−52.323	−52.322		
16	18 316	−56.816	−56.816		
17	48 458	−61.318	−61.318		
18	1.28×10^5	−66.531	−66.531		
19	3.39×10^5	−72.660	−72.660	−70.077	−72.660

[a]Estimated number of minima for n atom cluster $m(n)=0.003\,180\,1\times\exp(0.9729n)$ based on data for $8\leqslant n\leqslant13$.
[b]Reference 44.
[c]Reference 45.

to sample whole regions of the potential hypersurface at each point in time. At each point in time, the MD phase point is able to sample the potential energy surface only at a single point. Using MD, a trajectory must be followed for some time before it samples a region of the potential as well as the GPP without moving. The far greater rate of annealing possible for the GPP algorithm is an indication of the greater effectiveness of the GPP in sampling the potential hypersurface.

IV. DISCUSSION

We have presented an approximate method for integrating the classical Liouville equation for the time evolution of the phase space density distribution using Gaussian phase packets. For an N-body system, one must solve $(2d+3)N$ equations of motion rather than the $2dN$ equations of standard molecular dynamics. However, as GPP dynamics results in the evolution of a volume of phase points, the sampling is generally enhanced over standard molecular dynamics algorithms which provide information for a single phase point. In our simulations, we found equipartitioning takes place significantly faster for the Gaussian phase packets than for standard molecular dynamics. The radial distribution functions were reasonably accurate at low to moderate temperatures, but showed somewhat too much structure at higher temperatures. While the equipartitioning between kinetic and potential energy is accurate for the GPP, differences in the radial distribution functions will manifest themselves in other thermodynamic properties such as the compressibility factor $Z=pV/nRT$. Moreover, we have demonstrated the efficiency of our global optimization algorithm based on simulated annealing of Gaussian phase packets. We found that the optimized annealing rate is much faster than is possible using standard MD.

The simulation of Gaussian phase packets is a first step towards more accurate solution of the Liouville equation. In a related work, Kay has derived a systematic mobile basis set expansion approach to solving the time-dependent Schrödinger equation based on the Hermite polynomials and the Dirac–Frenkel variational principle.[35] This approach may be easily adapted for the Liouville equation. The algorithm becomes numerically stiff rather quickly as the basis size increases; however, it is possible only modest basis sizes may be needed.

It is worth mentioning that there are alternative methods for applying the constant temperature constraint to our equations of motion. We begin with the kinetic equation[36,37]

$$\left(\frac{\partial}{\partial t}+L_0\right)\rho(r,p,t)=-L_c\rho(r,p,t), \tag{43}$$

where L_0 is the standard "streaming" Liouville operator of Eq. (3) and L_c represents the "collision" operator which introduces effects of the bath. Alternatively, the collision operator may be expressed as a continuous master equation.[37,38] For our constant temperature algorithm, we use

$$L_c=-\gamma\frac{\partial}{\partial p}\cdot p \tag{44}$$

coupled with an external constraint equation which adjusts γ to hold the temperature rigorously constant. This constraint was inspired by the work of Hoover and Evans.[39] However, following the hybrid constant temperature algorithm of Andersen,[40] one might choose a BGK-like collision operator[36,37,41]

$$L_c=\gamma\left[1-\left(\frac{m}{2\pi k_BT}\right)^{d/2}\exp(-p^2/2mk_BT)\int dp\right] \tag{45}$$

which thermalizes the momentum with a rate γ according to the Maxwell distribution. In our GPP dynamics algorithm, this corresponds to integrating deterministic dynamics specified by Eq. (18), where only the equation of motion for $M_{0,2}$ is replaced by

$$\dot{M}_{0,2}=-\frac{2}{d}M_{1,1}\nabla_{r_0}^2\langle V\rangle-\gamma[M_{0,2}-(p_0^2+dmk_BT)]. \tag{46}$$

The "collision" frequency γ is a constant which may be chosen to reproduce the diffusion constant or viscosity of the system. Note that constant temperature BGK-*molecular dynamics* consists of a random process of thermalization of the particle velocity with a frequency of γ. However, using GPP, the dynamics is continuous and deterministic. The system temperature fluctuates about the chosen "bath" temperature and the fluctuation size is controlled by the magnitude of γ. In fact, the term in the equation of motion for $M_{0,2}$ proportional to γ has the form of an effective harmonic restoring force acting on $M_{0,2}$ to constrain it about an equilibrium value of $p_0^2+dmk_BT$. In this way, the algorithm is similar to that of Nosé and Hoover, where the temperature is controlled via coupling of the system to an external thermostat.[42,43]

ACKNOWLEDGMENTS

We thank Carmay Lim and David Coker for helpful discussions. D.H. thanks David Coker for support. This work was supported in part by a grant from the American Chemical Society's Petroleum Research Fund, and in part by a grant from the National Science Foundation (Grant No. CHE-9306375).

APPENDIX A: DERIVATION OF EQ. (5)

The moments of the classical density distribution in position and momentum are defined as

$$\begin{aligned}M_{n,k}&=\langle(r-r_0)^n(p-p_0)^k\rangle,\\ W_{n,k}&=\langle(r-r_0)^n(p-p_0)^k(F-F_0)\rangle,\end{aligned} \tag{A1}$$

where $\langle\cdots\rangle$ denotes an average over the classical phase space density distribution $r_0=\langle r\rangle$, $p_0=\langle p\rangle$, and $F_0=\langle F(r)\rangle$. For example,

$$\langle (r-r_0)^n (p-p_0)^k \rangle = \int d^d r \int d^d p (r-r_0)^n \times (p-p_0)^k \rho(r,p,t). \quad \text{(A2)}$$

The time evolution of the phase space density distribution function obeys the Liouville equation

$$\frac{\partial}{\partial t}\rho(r,p,t) = -L_0 \rho(r,p,t), \quad \text{(A3)}$$

where L_0 is the Liouville operator

$$L_0 = \frac{p}{m}\cdot\frac{\partial}{\partial r} + F(r)\cdot\frac{\partial}{\partial p}. \quad \text{(A4)}$$

Taking the time derivative of $M_{n,k}$, substituting $\dot{p} = -L_0 p$ and integrating that term by parts, we find

$$\frac{\partial M_{n,k}}{\partial t} = \int d^d r \int d^d p \left(L_0 + \frac{\partial}{\partial t}\right)(r-r_0)^n (p-p_0)^k \rho(r,p,t)$$
$$= \int d^d r \int d^d p \left[\frac{p}{m} n (r-r_0)^{n-1}(p-p_0)^k + k(r-r_0)^n (p-p_0)^{k-1} F(r) + n(r-r_0)^{n-1}(-\dot{r}_0)(p-p_0)^k + k(r-r_0)^n (-\dot{p}_0)(p-p_0)^{k-1}\right]\rho(r,p,t), \quad \text{(A5)}$$

where we have used the fact that $d\rho(r,p,t)/dt = 0$.

Inserting the identities $\dot{r}_0 = p_0/m$ and $\dot{p}_0 = F_0$, and collecting the moments, we find the final result

$$\frac{\partial M_{n,k}}{\partial t} = \frac{n}{m} M_{n-1,k+1} + k W_{n,k-1} \quad (5)$$

which is an exact equation of motion for the hierarchy of moments of the classical density distribution.

APPENDIX B: DERIVATION OF EQ. (25)

In the calculation of pair correlation functions, one requires the collective probability that given a particle at coordinate $\mathbf{r}^{(1)}$, there is another particle a distance $|\mathbf{r}|$ away. (For this discussion, we temporarily revert to explicit vector notation.) To calculate this function, we first calculate the probability of finding the second particle at the coordinate $\mathbf{r}^{(2)}$ with $\mathbf{r} = \mathbf{r}^{(1)} - \mathbf{r}^{(2)}$,

$$P(\mathbf{r}) = \int d\mathbf{p}^{(1)} \int d\mathbf{p}^{(2)} \int d\mathbf{r}^{(1)} \int d\mathbf{r}^{(2)} \rho^{(1)}(\mathbf{r}^{(1)},\mathbf{p}^{(1)}) \rho^{(2)}(\mathbf{r}^{(2)},\mathbf{p}^{(2)}) \delta(\mathbf{r}^{(1)} - \mathbf{r}^{(2)} - \mathbf{r})$$
$$= \int d\mathbf{p}^{(1)} \int d\mathbf{p}^{(2)} \int d\mathbf{r}^{(1)} \rho^{(1)}(\mathbf{r}^{(1)},\mathbf{p}^{(1)}) \rho^{(2)}(\mathbf{r}^{(1)} - \mathbf{r},\mathbf{p}^{(2)})$$
$$= \left(\frac{\zeta}{\pi}\right)^{3/2} \exp[-\zeta(\mathbf{r}-\mathbf{r}_{12})^2], \quad \text{(B1)}$$

where the last line depends on the distribution being Gaussian, and $\zeta = d/[2(M_{2,0}^{(1)} + M_{2,0}^{(2)})]$, $\mathbf{r}_{12} = \mathbf{r}_0^{(1)} - \mathbf{r}_0^{(2)}$, and $\mathbf{r}_0^{(1)}$ and $\mathbf{r}_0^{(2)}$ represent the density distribution centers of particles 1 and 2. From this expression, we constrain the interparticle separation to a magnitude $r = |\mathbf{r}|$ to calculate the probability

$$G(r) = \int d\mathbf{r}\, P(\mathbf{r}) \delta(|\mathbf{r}| - r) \quad \text{(B2)}$$

which is defined for $0 \leqslant r < \infty$. Integrating over the angular variables (where it is simplest to take $\mathbf{r}_{12} = r_{12}\hat{z}$ and $(\mathbf{r}-\mathbf{r}_{12})^2 = r^2 + r_{12}^2 - 2rr_{12}\cos\theta$) provides us with the final result

$$G(r) = \left(\frac{\zeta}{\pi}\right)^{1/2} \frac{r}{r_{12}} \{\exp[-\zeta(r-r_{12})^2] - \exp[-\zeta(r+r_{12})^2]\} \quad (25)$$

for the probability of finding particles 1 and 2 a radial distance r apart when the density distribution of each particle is represented using spherically symmetric Gaussian phase packets.

[1] M. P. Allen and D. J. Tildesley, *Computer Simulation of Liquids* (Oxford, Bristol, 1990).
[2] C. L. Brooks, M. Karplus and M. Pettitt, *Proteins: A Theoretical Perspective of Dynamics, Structure, and Thermodynamics* (Wiley, New York, 1988).
[3] J. A. McCammon and S. C. Harvey, *Dynamics of Proteins and Nucleic Acids* (Cambridge University, New York, 1987).

[4] J. E. Straub and D. Thirumalai, Proc. Natl. Acad. Sci. USA **90**, 809 (1993); J. E. Straub and D. Thirumalai, Proteins **15**, 360 (1993).
[5] F. H. Stillinger and T. A. Weber, Phys. Rev. A **25**, 978 (1982); **28**, 2408 (1983); Science **225**, 983 (1984).
[6] H. Frauenfelder, S. G. Sligar, and P. G. Wolynes, Science **254**, 1598 (1991); H. Frauenfelder, F. Parak, and R. D. Young, Annu. Rev. Biophys. Chem. **17**, 451 (1988).
[7] R. Elber and M. Karplus, J. Am. Chem. Soc. **112**, 9161 (1990); R. Czerminski and R. Elber, Proteins **10**, 70 (1991).
[8] B. J. Berne and R. Pecora, *Dynamic Light Scattering* (Wiley-Interscience, New York, 1976).
[9] E. J. Heller, J. Chem. Phys. **62**, 1544 (1975); Acc. Chem. Res. **14**, 368 (1981).
[10] D. Thirumalai, E. Bruskin, and B. J. Berne, J. Chem. Phys. **83**, 230 (1985).
[11] R. D. Coalson and M. Karplus, J. Chem. Phys. **79**, 6150 (1983); **81**, 2891 (1984); **93**, 3919 (1990); see also A. D. McLachlan, Mol. Phys. **8**, 39 (1964); E. J. Heller, J. Chem. Phys. **64**, 63 (1976).
[12] S. Mukamel, J. Phys. Chem. **88**, 3185 (1984).
[13] J. Grad, Y. J. Yan, A. Haque, and S. Mukamel, Chem. Phys. Lett. **134**, 219 (1987); J. Chem. Phys. **86**, 3441 (1987).
[14] Y. J. Yan and S. Mukamel, J. Chem. Phys. **88**, 5735 (1988); S. Mukamel and Y. J. Yan, Adv. Chem. Phys. **73**, 579 (1989).
[15] In the respect that our goal is to simulate many-body systems, our work is closely related to the work of N. Corbin and K. Singer, Mol. Phys. **46**, 671 (1982); and K. Singer and W. Smith, *ibid.* **57**, 761 (1986), who apply Gaussian wave packets to the quantum simulation of neon atoms in real time.
[16] Related in spirit to this work is an intriguing method of global optimization based on the classical density distribution expanded as a Gaussian by D. Shalloway, in *Recent Advances in Global Optimization*, edited by A. Floudas and P. M. Pardalos (Princeton University, Princeton, 1992), p. 433.
[17] The classical trajectory-bundle TDSCF method provides greater flexibility than Gaussian wave packets at the cost of introducing more degrees of freedom; see R. B. Gerber and M. A. Ratner, Adv. Chem. Phys. **70**, 97 (1988); G. C. Schatz, V. Buch, M. A. Ratner, and R. B. Gerber, J. Chem. Phys. **79**, 1808 (1983); V. Buch, R. B. Gerber, and M. A. Ratner, Chem. Phys. Lett. **101**, 44 (1983); R. B. Gerber, V. Buch, and M. A. Ratner, J. Chem. Phys. **77**, 3022 (1982); Chem. Phys. Lett. **91**, 173 (1982).
[18] R. C. Tolman, *The Principles of Statistical Mechanics* (Dover, New York, 1979).
[19] R. W. Zwanzig, in *Lectures in Theoretical Physics*, edited by W. E. Britton, B. W. Downs, and J. Downs (Wiley-Interscience, New York, 1961), p. 106; see also, J. Chem. Phys. **33**, 1338 (1960).
[20] J. Frenkel, *Wave Mechanics: Advanced General Theory* (Clarendon, Oxford, 1934); in the Dover edition (1950), see p. 253; Frenkel cites an appendix in the Russian edition of Dirac's *Principles of Quantum Mechanics* (1930).
[21] We have described earlier how the many-body density distribution may be expanded as a product of Gaussian phase packets. For the special case when each particle is represented by a single Gaussian with mean squared width $M_{2,0}$, the resulting equations of motion are for a Gaussian whose center in position space moves over an averaged effective pair potential. The effective potential for the center of the Gaussian r_0 is identical to the deformed interaction potential employed in the diffusion equation method of L. Piela, J. Kostrowicki and H. A. Scheraga, J. Phys. Chem. **93**, 3339 (1989) for finding the global minimum of a potential surface. The squared width of the Gaussian $M_{2,0}$ is proportional to their diffusion "time."
[22] W. G. Hoover, A. J. C. Ladd and B. Moran, Phys. Rev. Lett. **48**, 1818 (1982); D. J. Evans, J. Chem. Phys. **78**, 3297 (1983).
[23] A. D. McLachlan, Mol. Phys. **8**, 39 (1964).
[24] J. S. Bader, R. A. Kuharski, and D. Chandler, J. Chem. Phys. **93**, 230 (1990).
[25] R. D. Mountain and D. Thirumalai, J. Phys. Chem. **93**, 6975 (1989).
[26] A. Messiah, *Quantum Mechanics* (Wiley, New York, 1976), Vol. 1.
[27] J. Kostrowicki, L. Piela, B. J. Cherayil, and H. A. Scheraga, J. Phys. Chem. **95**, 4113 (1991).
[28] K. D. Gibson and H. A. Scheraga, in *Structure and Expression: From Proteins to Ribosomes*, edited by M. H. Sarma and R. H. Sarma (Adenine, Schenectady, NY, 1988).
[29] L. Piela, J. Kostrowicki, and H. A. Scheraga, J. Phys. Chem. **93**, 3339 (1989); J. Kostrowicki, L. Piela, B. J. Cherayil, and H. A. Scheraga, *ibid.* **95**, 4113 (1991); J. Kostrowicki and H. A. Scheraga, *ibid.* **96**, 7442 (1992).
[30] K. A. Olszewski, L. Piela, and H. A. Scheraga, J. Phys. Chem. **96**, 4672 (1992); **97**, 260 (1993); **97**, 267 (1993).
[31] R. Somorjai, J. Phys. Chem. **95**, 4141 (1991); **95**, 4147 (1991).
[32] P. Amara, D. Hsu, and J. E. Straub, J. Phys. Chem. **97**, 6715 (1993).
[33] J. Ma, P. Amara, and J. E. Straub, J. Chem. Phys. (to be published).
[34] S. Kirkpatrick, Jr., C. D. Gelatt, and M. P. Vecchi, Science **220**, 671 (1983).
[35] K. G. Kay, J. Chem. Phys. **91**, 170 (1989); Chem. Phys. **137**, 165 (1989); see also D. Hsu and D. Coker, J. Chem. Phys. **96**, 4266 (1992); **97**, 5931 (1992).
[36] J. L. Skinner and P. G. Wolynes, J. Chem. Phys. **69**, 2143 (1978).
[37] J. L. Skinner and P. G. Wolynes, J. Chem. Phys. **72**, 4913 (1980).
[38] B. J. Berne, *Multiple Time Scales*, edited by J. U. Brackbill and B. I. Cohen (Academic, New York, 1985).
[39] D. J. Evans, W. G. Hoover, B. H. Failor, B. Moran, and A. J. C. Ladd, Phys. Rev. A **28**, 1016 (1983).
[40] H. C. Andersen, J. Chem. Phys. **72**, 2384 (1980).
[41] B. J. Berne, J. L. Skinner, and P. G. Wolynes, J. Chem. Phys. **73**, 4314 (1980).
[42] S. Nosé, J. Chem. Phys. **81**, 511 (1984).
[43] W. G. Hoover, Phys. Rev. A **31**, 1695 (1985).
[44] M. R. Hoare, Adv. Chem. Phys. **40**, 49 (1979).
[45] J. A. Northby, J. Chem. Phys. **87**, 6166 (1987).